BIOCHEMISTRY
including biophysical chemistry & molecular biology
Article

Biochemistry **2009,** *48,* 3887–3893 3887
DOI:10.1021/bi802362t

Effects of Tyrosine Mutations on the Conformational and Oxidative Folding of Ribonuclease A: A Comparative Study†

Robert F. Gahl, Lovy Pradeep, Corey R. Siegel, Guoqiang Xu, and Harold A. Scheraga*

Baker Laboratory of Chemistry, Cornell University, Ithaca, New York 14853

Received December 28, 2008. Revised Manuscript Received March 6, 2009

ABSTRACT: Ribonuclease A (RNase A) undergoes more rapid conformational folding with its disulfide bonds intact than during oxidative folding from its reduced form. In this study, the effects of the mutants Y92G, Y92A, and Y92L on both the conformational and oxidative folding pathways were examined to determine the role of native interactions in different types of conformational searches for the biologically active structure of a protein. These mutations did not affect the overall conformational folding pathway of RNase A. However, in the mutants Y92G and Y92A, a key structured disulfide-bonded species, des-[65−72], involved in the oxidative folding pathway of RNase A, was destabilized. These results demonstrate the importance of native interactions in the folding process, namely, protection of a native (40−95) disulfide bond by a nearby tyrosyl−prolyl stacking interaction, when disulfide bonds are allowed to undergo SH/S−S reshuffling.

The process of how the four-disulfide-bond-containing protein RNase A[1] obtains its biologically active or native structure from an unfolded state has been studied extensively (*1*−*9*). The goal of these studies was to understand how interactions among amino acids drive the conformational search to fold a protein into its native structure. Acquiring native structure in disulfide-intact proteins is termed conformational folding. Acquiring native structure, in addition to the correct disulfide bond linkages in the presence of an oxidizing agent from a state in which the disulfide bonds are reduced, is termed oxidative folding. The goal of this study is to understand how these two different folding mechanisms utilize some of the same native interactions. In the conformational space that is searched in the disulfide-intact folding mechanism, disulfide bonds restrict the freedom of the backbone, and as a result, folding takes place in minutes. In oxidative folding, the backbone is less restricted and the search of conformational space is influenced by the formation of disulfide bonds. In contrast to conformational folding, oxidative folding takes place in hours. Therefore, the degree to which the same side chain−side chain interactions drive the folding process is different in these two types of folding mechanisms.

The conformational folding pathway of RNase A has been studied extensively in many laboratories (*1*−*4*) and in our own (*5*−*7*). An equilibrium population of different unfolded states appears in GdnHCl-denatured RNase A, U-RNase A, because of proline isomerization (*10*,*11*); each state folds concomitantly to N at different rates when the GdnHCl is rapidly diluted to impose folding conditions.

The oxidative folding mechanism by which RNase A concomitantly attains its correct disulfide linkages as well as its biologically active structure has been identified (*8*,*9*) (Figure 1). In the presence of the redox couple, DTT^{ox}/DTT^{red}, a pre-equilibrium is first established among unstructured ensembles that contain zero, one, two, three, or four native and non-native disulfide bonds. Through a redox-independent SH/S−S reshuffling step, two structured species, des-[65−72] and des-[40−95] (*8*,*9*), are preferentially populated from the unstructured 3S ensemble in the rate-determining step along two different pathways (*8*,*9*) and then oxidized rapidly to N-RNase A.

To observe how these two mechanisms may differ in their utilization of side chain−side chain interactions, tyrosine 92 was mutated to remove a ring stacking interaction with proline 93, and the extent of the effect of this mutation on the oxidative folding and conformational

*To whom correspondence should be addressed. Telephone: (607) 255-4034. Fax: (607) 254-4700. E-mail: has5@cornell.edu.

†This research was supported by NIH Grant GM-24893.

[1]Abbreviations: RNase A, wild-type bovine pancreatic ribonuclease A; N-x-RNase A, RNase A for which N indicates that native disulfide bonds are intact and x indicates a Y92 mutant or wild-type protein; R-RNase A, RNase A without disulfide bonds; U-RNase A, disulfide-intact RNase A denatured by GdnHCl; $3S_U$, unstructured ensemble of species containing three native and/or non-native disulfide bonds; $3S_F$, three-disulfide structured species with only native disulfide bonds; des-[*x*−*y*], disulfide-bond species that contains native disulfide bonds except for the *x*−*y* disulfide bond; GdnHCl, guanidine hydrochloride; TFA, trifluoroacetic acid; Tris, tris(hydroxymethyl)aminomethane; DTT^{ox} and DTT^{red}, oxidized and reduced forms, respectively, of dithiothreitol; EDTA, ethylenediaminetetraacetic acid; PCR, polymerase chain reaction; RP-HPLC, reversed-phase high-performance liquid chromatography.

Published on Web 4/3/2009

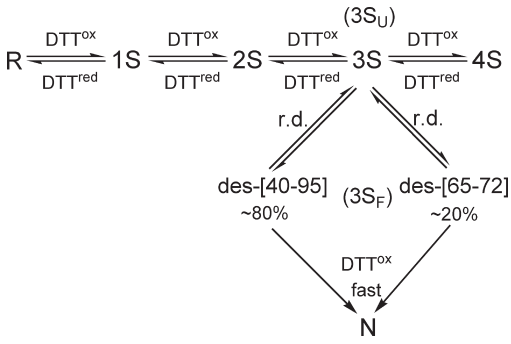

FIGURE 1: Oxidative folding mechanism of RNase A at 25 °C (*9*). The role of $3S_U$ and $3S_F$ in the rate-determining step in the mechanism is indicated.

folding pathways relative to those of wild-type RNase A is measured and compared to that of the wild-type protein.

Previous work (*12*,*13*) with mutations of tyrosine 92 showed that they affect the redox chemistry around the [40−95] disulfide bond. In the crystal structure (*14*) in Figure 2, Y92 and P93 form a ring stacking interaction in which the tyrosine residue covers the (40−95) disulfide bond. When the Y92 residue is removed in the mutants, the (40−95) disulfide bond becomes more exposed. In a previous study (*13*), the mutation of Y92 to G, A, or L affected the reductive unfolding pathway of RNase A in which the [40−95] disulfide bond was preferentially reduced over the (65−72) disulfide bond; i.e., the rate of reduction of the (40−95) disulfide bond is increased, and des-[40−95] is the only three-disulfide bond species observed on the reductive unfolding pathway. For wild-type RNase A, both the (40−95) and (65−72) disulfide bonds are reduced along two different reductive unfolding pathways (*15*). Because the [40−95] disulfide bond can be more easily reduced in the mutants, the oxidative folding of mutant RNase A is also affected. The Y92G mutant of RNase A recovers its biologically active form more slowly than WT RNase A (*12*). A similar increase in the reducibility of the (40−95) disulfide bond is also observed in the P93A mutant (*16*). In this mutant, the ring stacking interaction was not present to help residue Y92 protect the (40−95) disulfide bond, thus making the latter more reactive.

To compare a conformational search between the oxidative folding mechanism and the disulfide-intact folding mechanism, we studied the effects of these mutants on the redox-independent reshuffling of the 3S ensemble of native and non-native disulfide bonds to des-[65−72] and des-[40−95]. In this step of the oxidative folding pathway of WT RNase A (Figure 1), the unstructured ensemble, $3S_U$, undergoes SH/S−S reshuffling along two different pathways to populate des-[65−72] and des-[40−95], both of which have nativelike structure (*17*,*18*), and oxidizes rapidly to form N-RNase A. In the rate-determining step that forms nativelike structure in the oxidative folding pathway (*9*), the $3S_U \rightarrow 3S_F$ reaction involves reshuffling but no oxidation or reduction. Our focus was placed here on the conformational folding in the transition from $3S_U$ to $3S_F$. Therefore, the effects of these mutants on this conformational folding in oxidative folding pathways can be compared with the conformational folding of disulfide-intact folding pathways.

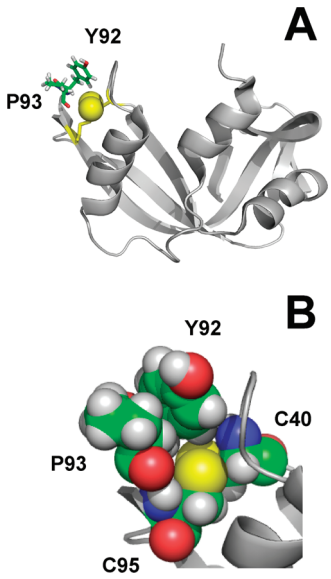

FIGURE 2: (A) Crystal structure of RNase A (Protein Data Bank entry 7RSA) (*14*), with Y92 and P93 in a green "stick" model and the sulfurs of the (40−95) disulfide bond colored yellow in a space filling model. (B) Close-up view of residues Y92, P93, C40, and C95 in a space filling model.

MATERIALS AND METHODS

Materials. Desired mutations in RNase A were achieved by PCR using the QuikChange site-directed mutagenesis kit from Stratagene. The required designed primers for PCR were obtained from Sigma-Genosys.

GdnHCl, required for unfolding of the proteins in kinetic studies, was obtained from Mallinckrodt Chemicals. Tris(hydroxymethyl)aminomethane hydrochloride (TRIZMA HCl, 99.9%), used in pH 8 buffers for kinetic studies, was obtained from Sigma-Aldrich. EDTA, used in buffers for kinetic studies, was obtained from Fischer Scientific. All other materials were obtained as the highest grade available.

Expression and Purification of WT RNase A and Y92 Mutants. Mutant primers were designed for site-directed Y92 substitutions to generate DNA plasmids for the RNase A mutants by PCR. The plasmid for wild-type RNase A in a pET22b(+) vector, obtained from previous studies (*19*), was used as a template for PCR along with the mutant primers. The protocol for PCR was taken from the QuikChange site-directed mutagenesis kit from Stratagene. Post-PCR, the sequencing of all the resultant mutant DNA plasmids was carried out at the Cornell Biotechnology Resource Center. The plasmid DNAs for the correct desired tyrosine-to-leucine, tyrosine-to-alanine, and tyrosine-to-glycine substitutions were used for protein overexpression and purification. Wild-type RNase A (type 1-A, Sigma-Aldrich) was purified by ion exchange chromatography (*13*). The protocols for the overexpression and purification of the mutant proteins from inclusion bodies have been described previously (*19*).

Preparation of $3S_U$ Ensembles of Wild-Type RNase A and Y92 Mutants. $3S_U$ ensembles of RNase A and Y92 mutants were produced by first populating a three-disulfide-bond-containing intermediate species from reductive unfolding of each protein. For wild-type RNase

A, the two species from N-WT-RNase A each with three native disulfide bonds, des-[65−72] and des-[40−95], were produced by incubating N-WT-RNase A in a 0.1 M Tris buffer at a concentration of 1 mg/mL at 15 °C for 12 h at pH 8.0 in the presence of 100 mM DTT^{red} (*15*). For the Y92A mutant, the des-[40−95] species from N-Y92A-RNase A was produced by incubating N-Y92A-RNase A under the same conditions that were used for wild-type RNase A except at a concentration of 0.5 mg/mL for 160 min (*13*). For the Y92G mutant, N-Y92G-RNase A was incubated under the same conditions used for N-Y92A-RNase A except that the reductive unfolding was allowed to proceed for 50 min (*13*). After the reductive unfolding reaction proceeded for the prescribed amount of time for each protein, the reaction was quenched by addition of glacial acetic acid.

The species of each protein with three native disulfide bonds was purified from the reductive unfolding mixtures by RP-HPLC using a water/acetonitrile buffer system with 0.09% TFA using a 25 cm × 4.6 mm SULPELCO Discovery BIO Wide Pore C18, 5 μm particle size column with the eluted species monitored at 210 nm. In the procedure used, buffer salts, DTT^{red}, and DTT^{ox} eluted first with an 85% water/15% acetonitrile mixture, followed by the protein using a gradient from 25 to 34% acetonitrile over 55 min. This gradient was sufficient to separate des-[65−72] and des-[40−95] from each other and from the native and reduced forms of both Y92A-RNase A and Y92G-RNase A. All of these purified species were collected separately, frozen, and lyophilized to remove TFA, water, and acetonitrile. After lyophilization, each of these three-disulfide species was reconstituted in 50 mM acetic acid and stored at −70 °C.

To generate an unstructured ensemble, $3S_U$, of Y92A-RNase A and Y92G-RNase A, the solutions of purified des-[40−95] from Y92A-RNase A and Y92G-RNase A were scrambled separately from the $3S_U$ ensemble by incubating the solutions of des-[40−95] from each protein in a pH 8.2, 0.1 M Tris buffer containing 5.6 M GdnHCl for 2 h over humidified argon at a protein concentration of 0.5 mg/mL to allow SH/S−S reshuffling to form non-native disulfide bonds. The $3S_U$ ensemble of WT-RNase A was generated similarly from des-[40−95] and des-[65−72] except that solutions containing purified des-[40−95] and des-[65−72] were combined before incubation in the same buffer. These buffer conditions, pH 8 and 5.6 M GdnHCl, are sufficient for unfolding the native forms of WT-RNase A, Y92A-RNase A, and Y92G-RNase A and, presumably, their less stable des species. The buffer containing 5.6 M GdnHCl was previously purged of oxygen with humidified argon. After 2 h, the SS/S−H reshuffling reaction was stopped by adding glacial acetic acid to lower the pH to 3. GdnHCl and buffer salts were removed from the scrambling mixtures on a G25 size-exclusion column equilibrated with 50 mM acetic acid, and the eluting species were monitored at 280 nm. Acetic acid was removed from the $3S_U$ ensemble by lyophilization. After lyophilization was complete, the $3S_U$ ensemble for each protein was reconstituted in 50 mM acetic acid at a concentration of 5 mg/mL and stored at −70 °C until further use.

Analyzing the Transition from the $3S_U$ Ensemble to the Mixture of Structured Species, $3S_F$, with Native Disulfide Bonds in the Wild Type and Y92 Mutants of RNase A. The $3S_U$ to $3S_F$ transition was initiated by diluting a 5 mg/mL stock solution of $3S_U$ with a 0.1 M Tris buffer (pH 8.0), previously purged of oxygen with humidified argon, to a final protein concentration of 0.5 mg/mL, and the transition was allowed to proceed for 40 min at pH 8.0 under humidified argon, with the reaction progress determined every 5 min.

To determine the amount of structured species that was present in the reaction mixture at different times, quantitatively, an aliquot was removed and subjected to a reduction pulse (*8*) with 5 mM DTT^{red}. The 5 mM DTT^{red} was allowed to reduce the unstructured three-disulfide-bond-containing species for 2 min to the reduced form of each of the proteins, and the reduction was then quenched with glacial acetic acid and stored frozen at −70 °C until it was analyzed by RP-HPLC. Under these conditions, structured three-disulfide-bond-containing species are not reduced by DTT^{red}. Each of the aliquots (at different reshuffling times) was analyzed by RP-HPLC as described above. The progress of the transition was followed quantitatively by integrating the area under the chromatographic curves of the structured species and the reduced protein, with the reduced protein corresponding to the unstructured species that were reduced by DTT^{red} during the reduction pulse. The species involved in the transition, the $3S_F$ species and R, were detected at 210 nm, and we assumed each had the same absorptivity because, under the conditions of separation by RP-HPLC, all the species were unfolded. Using the precautions against oxidation by oxygen for the duration of the experiment, a maximum air oxidation of species of no more than 3% was observed.

According to the mechanism in Figure 1, the system of differential equations that describes the formation of two structured $3S_F$ species from the unstructured $3S_U$ ensemble is as follows:

$$\frac{d[3S_U]}{dt} = -(k_1 + k_2)[3S_U] \quad (1)$$

$$\frac{d[3S_{F_1}]}{dt} = k_1[3S_U] \quad (2)$$

$$\frac{d[3S_{F_2}]}{dt} = k_2[3S_U] \quad (3)$$

where k_1 and k_2, and F_1 and F_2, correspond to the two structured des species.

The analytical solution for this system of differential equations is as follows:

$$[3S_U(t)] = [3S_U]_0 e^{-(k_1+k_2)t} \quad (4)$$

$$[3S_{F_1}(t)] = \frac{k_1[3S_U]_0}{k_1 + k_2}[1 - e^{-(k_1+k_2)t}] \quad (5)$$

$$[3S_{F_2}(t)] = \frac{k_2[3S_U]_0}{k_1 + k_2}[1 - e^{-(k_1+k_2)t}] \quad (6)$$

where $[3S_U]_0$ is the initial concentration of $3S_U$. For WT-RNase A, as shown in Figure 1, the two structured $3S_F$ species are des-[65−72] and des-[40−95]. The progress of this reaction was followed quantitatively by using RP-HPLC to calculate the relative fraction of each species, with the quantity $[3S_U]_0$ taken to be 1.0.

While it was shown previously (*15*) that these two $3S_F$ species have a tendency to reshuffle back to the unstructured $3S_U$ ensemble, the rate of this back-reshuffling from $3S_F$ to $3S_U$ is much slower than the rate of reshuffling of the $3S_U$ ensemble to the $3S_F$ species (*15*). This was verified by obtaining the solutions of the system of differential equations, eqs 1−3, with and without additional back-reshuffling reactions for the $3S_F$ species. There was no discernible difference between the time-dependent concentrations of the two $3S_F$ species with and without back-reshuffling, within the time used to study this transition. Therefore, the back-reshuffling of the $3S_F$ species to the $3S_U$ ensemble was not taken into account in this analysis.

To identify the $3S_F$ species formed in the SH/S−S reshuffling of $3S_U$ to $3S_F$, the Wu−Watson cyanylation method was used to identify the free cysteines (*20*). The disulfide-bond connectivity of the wild-type and mutant forms was determined to be native because the $3S_F$ species produced in this transition for each of these proteins exhibit the same chromatographic behavior (*8*,*15*) as the corresponding species that are also populated in the reductive unfolding pathways of the native wild-type and mutant proteins.

Conformational Folding of Disulfide Bond-Intact Wild-Type RNase A and Y92 Mutants. All refolding studies were carried out at 15 °C to observe the entire kinetic processes by minimizing burst-phase kinetics, if any. All single-jump measurements on the native forms of the wild-type and Y92 mutant proteins, N-WT-RNase A, N-Y92G-RNase A, N-Y92A-RNase A, and N-Y92L-RNase A, were conducted on a stopped-flow mixing module from HI-TECH Scientific using absorbance at 287 nm as the optical probe. For refolding studies, the proteins were first unfolded in unfolding buffer [5.9 M GdnHCl, 0.1 M Tris, and 1 mM EDTA (pH 8.0)] at room temperature for 4 h prior to refolding to ensure complete unfolding and then equilibrated at 15 °C prior to the start of kinetic experiments on the stopped-flow mixing module. Each unfolded protein was diluted 11-fold in refolding buffer [0.1 M Tris and 1 mM EDTA (pH 8.0)] at 15 °C on the stopped-flow mixing module so that the final refolding condition was pH 8.0 and 0.53 M GdnHCl at 15 °C. The refolding kinetics were acquired on a log-time base in which the acquisition is faster on the millisecond time scale and slower on the second time scale, thereby allowing accurate measurements to be taken in the fast kinetics regime. The procedure described previously (*21*) was used to minimize viscosity effects and thereby ensure proper mixing at the cost of an increase in the dead time. An increase in the dead time did not give rise to any burst-phase kinetics since the mixings were carried out at 15 °C.

The observable refolding kinetics of the wild-type and Y92 mutant proteins under the conditions mentioned above are described by a four-exponential process when monitored by absorbance at 287 nm by the following equation:

$$a(t) = a(\infty) - a_1 e^{-k_1 t} - a_2 e^{-k_2 t} - a_3 e^{-k_3 t} - a_4 e^{-k_4 t} \quad (7)$$

where $a(t)$ and $a(\infty)$ are the observed amplitudes at times t and at infinite time, respectively, k_1, k_2, k_3, and k_4 are the rate constants of the fast, medium, slow, and very slow phases, respectively, and a_1, a_2, a_3, and a_4 are the respective amplitudes. The very fast phase cannot be distinguished from the fast phase in a single-jump experiment but can be in a double-jump experiment (*5*).

RESULTS

Effects of the Y92G and Y92A Mutants on the $3S_U$ to $3S_F$ Transition of RNase A. Analysis of the effects of these mutants should recognize the fact that the $3S_U$ to $3S_F$ transition was examined here, independent of the rest of the oxidative folding pathway shown in Figure 1. Irrespective of whether the $3S_U$ ensemble is populated in the oxidative folding pathway or is produced by the methods introduced here, it is still an unstructured ensemble; however, the distribution of species in the $3S_U$ ensemble, and the transition to $3S_F$, could differ between these two circumstances. When the $3S_U$ ensemble is populated in the oxidative folding pathway and participates in a pre-equilibrium, some of the species are reduced to populate the 2S ensemble or oxidized to populate the 4S ensemble. These redox reactions could affect the distributions of the $3S_U$ ensemble. There were no oxidizing or reducing agents present in the investigation carried out here. According to Table 1, there is a difference in the rate constant associated with the formation of the des-[40−95] species in this study [$(5.9 \pm 0.3) \times 10^{-3}$ min^{-1}] and that calculated in ref *9* [$(1.4 \pm 0.1) \times 10^{-2}$ min^{-1}]. However, there is essentially no difference in the rate constant associated with the formation of des-[65−72]; the value determined in this study was $(1.8 \pm 0.1) \times 10^{-3}$ min^{-1}, while that reported in ref *9* is $(2.1 \pm 0.2) \times 10^{-3}$ min^{-1}. This discrepancy in k_1 could arise from the presence of DTT^{ox} and DTT^{red} during oxidative folding, but their absence in this study of the isolated $3S_U$ to $3S_F$ reshuffling. Since des-[40−95] and des-[65−72] are formed from $3S_U$ in different pathways (*9*), with different inter-residue

Table 1: Rate Constants ($\times 10^2$ min^{-1}) for Formation of the Structured Species, des-[65-72] and des-[40-95], of Wild-Type RNase A and the Y92A and Y92G Mutants

	wild-type RNase A[a]	wild-type RNase A[b]	Y92A RNase A	Y92G RNase A
3S → des-[40−95] (k_1)[d]	0.59[c] ± 0.03	1.4[c] ± 0.1	0.70 ± 0.04	0.91 ± 0.06
3S → des-[65−72] (k_2)[d]	0.18 ± 0.01	0.21 ± 0.02	−	−

[a] Current study. [b] From ref *9*. [c] See Results for the discrepancy between these two values. [d] From eqs 4−6.

interactions in each pathway, it is possible that the absence of this discrepancy in the k_2 pathway is due to such different inter-residue interactions. Hence, given that the conformational search in the $3S_U$ ensemble in this study or in the oxidative folding pathway finds two structured species, des-[40−95] and des-[65−72], with rate constants k_1 and k_2 within the same magnitude, the results of this study can be applicable to effects in the oxidative folding pathway. Yet the effects of the mutants Y92A-RNase A and Y92G-RNase A on the conformational search within $3S_U$ should be compared to the results under the same conditions used for the wild-type protein; i.e., the conformational search within the $3S_U$ ensemble should be independent of the oxidative folding pathway.

The Y92A-RNase A and Y92G-RNase A mutants affect the $3S_U$ to $3S_F$ transition of RNase A such that only one $3S_F$ species is observed within the time scale of the reaction. However, within the same time scale, both des-[65−72] and des-[40−95] are observed for wild-type RNase A. Figure 3 shows three chromatograms for 24 min transitions of Y92A, Y92G, and wild-type RNase A. After SS/S−H reshuffling for 24 min, des-[65−72] and des-[40−95] are detectable for the wild-type protein, but only des-[40−95] is observed for the mutants Y92A and Y92G. As seen in Table 1, the rate constants calculated for the formation of des-[40−95], $(7.0 \pm 0.4) \times 10^{-3}$ min^{-1} for Y92A-RNase A and $(9.1 \pm 0.6) \times 10^{-3}$ min^{-1} for Y92G-RNase A, are comparable to the rate constant calculated for WT-RNase A [$(5.9 \pm 0.3) \times 10^{-3}$ min^{-1}]. A rate constant for the formation of the des-[65−72] species was not calculated for this species for each of the mutants, Y92A-RNase A and Y92G-RNase A, because des-[65−72] was not observed.

While the value of the rate constant for the formation of des-[65−72] in wild-type RNase A is much smaller than that for des-[40−95], the des-[65−72] species is still important for the formation of N-RNase A because 20% of the biologically-active form of RNase A is obtained from direct oxidation of des-[65−72] (*9*). This des species and des-[40−95] each have substantial nativelike structure (*17*,*18*). Therefore, the observation that this species is destabilized in these mutants is not trivial.

Effects of Mutants Y92A, Y92G, and Y92L on the Conformational Folding Pathway. These Y92 mutants affect local structure during the conformational folding pathway of disulfide-intact RNase A instead of disrupting more global structure as seen in the $3S_U$ to $3S_F$ transition. According to Figure 4, each protein, including the mutants and wild type, recovers the biologically-active form in the same amount of time. However, these mutations do affect the slow phase, U_S, involved in the conformational folding pathway because of the isomerization of Pro93 (*5*).

According to column 4 of Table 2, as the size of the side chain of the mutated residue became smaller in size, L → A → G, the time constant associated with the folding of the slow phase decreases, which corresponds to an increase in the rate of folding for this phase. With the decrease in the size of the side chain that interacts with Pro93, Pro93 isomerizes at an increased rate because the steric hindrance between this residue and the side chain at residue 92 is lower. Since isomerization of Pro93 from the non-native *trans* conformer to the native *cis* conformer is a rate-limiting event in the folding of the U_S phase, an increase in the rate of isomerizaiton leads to an increase in the rate of folding for the U_S phase. Slower isomerization of Pro93 due to steric hindrance and accompanying slower rates of folding can be seen in the slow-phase folding in WT-RNase A and the large leucine mutant,

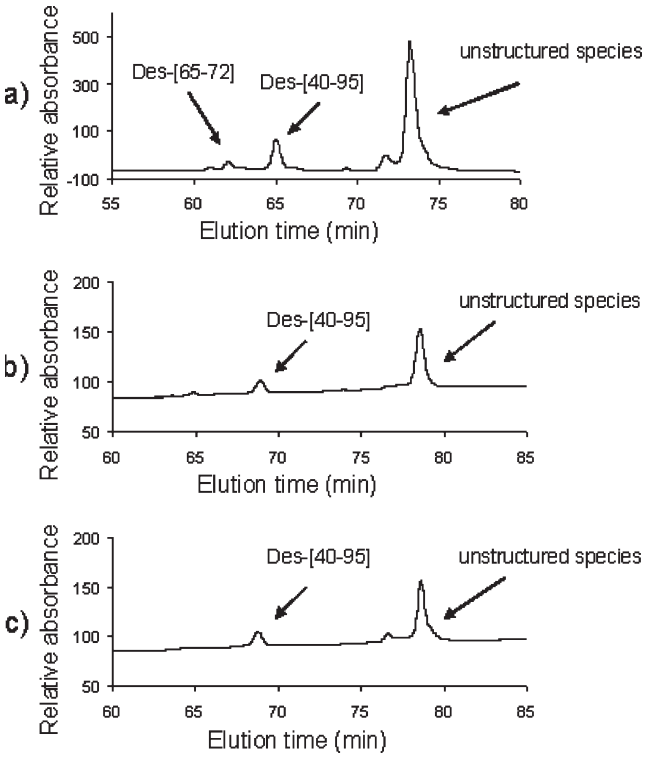

FIGURE 3: Elution profiles of the $3S_U$ to $3S_F$ transition at 25 °C and pH 8.0 for WT-RNase A (a), Y92G-RNase A (b), and Y92A-RNase A (c). Each of these profiles shows the progress of the $3S_U$ to $3S_F$ transition after 24 min. The elutions of the des species, des-[65−72] and des-[40−95], and the reduced unstructured species are indicated.

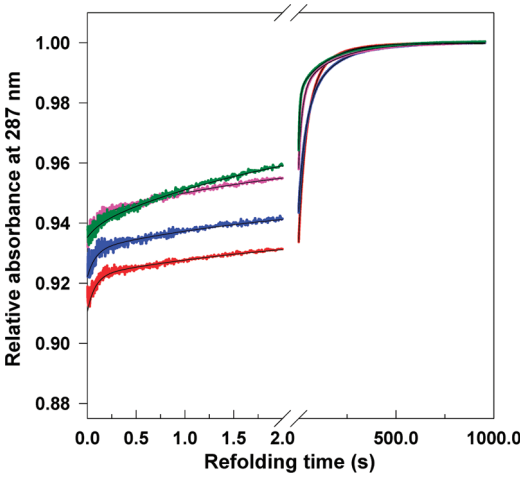

FIGURE 4: Single-jump kinetics of refolding at pH 8 and 15 °C. Representative normalized kinetic traces of refolding, monitored by absorbance at 287 nm for wild-type (red), Y92L (blue), Y92A (magenta), and Y92G (green) RNase A proteins, at a final refolding GdnHCl concentration of 0.53 M. The solid lines through the data are fits to eq 7 with the parameters listed in Table 2.

Table 2: Kinetic Parameters (for each observable phase) in the Single-Jump Refolding of the Wild-Type and Y92 Mutant RNase A Proteins at pH 8, 0.53 M GdnHCl, and 15 °C

Y92 mutant of RNase A	fast phase	medium phase	slow phase	very slow phase
		Time Constants, τ (s)		
wild type	0.041 ± 0.03	1.65 ± 0.15	38.85 ± 1.9	149.4 ± 9.0
Y92L	0.073 ± 0.02	1.54 ± 0.14	34.64 ± 2.2	192.2 ± 36.0
Y92A	0.070 ± 0.04	1.49 ± 0.27	19.62 ± 2.3	187.3 ± 57.4
Y92G	0.086 ± 0.03	1.65 ± 0.16	8.12 ± 1.5	163.3 ± 58.5
		Relative Amplitudes, *a* (%)		
wild type	10.62 ± 0.77	49.73 ± 9.6	19.70 ± 2.4	19.92 ± 6.9
Y92L	15.05 ± 1.37	37.61 ± 9.3	32.69 ± 2.0	14.74 ± 8.4
Y92A	21.10 ± 1.84	38.24 ± 6.6	23.30 ± 1.7	17.46 ± 5.4
Y92G	12.04 ± 6.90	35.51 ± 4.1	21.78 ± 5.6	24.04 ± 1.6

Y92L-RNase A, with time constants similar in magnitude (column 4).

Despite these effects on the slow phase, the time constants and amplitudes of the other phases are unaffected by mutation of Y92, as seen in the rest of the columns in Table 2. The diversity of unfolded states that gives rise to different phases in the folding pathway is due to the isomerization states of different prolines in RNase A. In phases other than the slow phase, Pro93 is in its native *cis* state. Removing the tyrosyl−prolyl interaction with the *cis* Pro93 does not affect the rate of folding for the other phases. This means that this interaction is not critical to the conformational folding of disulfide-intact RNase A, and removing this interaction affects species that are only locally involved in the folding pathway.

DISCUSSION

While a structured intermediate in the mutants Y92A and Y92G is destabilized compared to that of the wild-type protein in the $3S_U$ to $3S_F$ transition, mutants Y92A, Y92G, and Y92L affect a species only in the unfolded state locally in the conformational folding pathway. Therefore, the $3S_U$ to $3S_F$ transition is more sensitive to changes in native interactions than the conformational folding pathway. Native interactions become more important when disulfide bonds are allowed to interchange rather than when they are fixed during the folding process.

As mentioned in the introductory section, Y92 and P93 form a ring-stacking interaction which shields and protects the (40−95) disulfide bond from reduction (*13*). In the $3S_U$ to $3S_F$ transition, thiolates attack disulfide bonds during the SH/S−S reshuffling. Therefore, this ring-stacking interaction can prevent reshuffling reactions from thiolates. To stabilize des-[65−72], each of its disulfide bonds, including the (40−95) disulfide bond, must be stabilized. Since this disulfide bond is stabilized by this ring-stacking interaction in the wild-type protein, removal of this ring-stacking interaction removes the extra protection of the (40−95) disulfide bond from thiolate attack. Once this ring-stacking interaction was removed, the (40−95) disulfide bond could not be stabilized and, thus, the structured species, des-[65−72] could not be populated within the time observed for this experiment during which the (40−95) disulfide bond is preferentially reduced. For des-[40−95], this species lacks the (40−95) disulfide bond, and protection of this disulfide bond is not required for its stabilization. As a result, des-[40−95] is observed in the $3S_U$ to $3S_F$ transition in the absence of this ring stacking interaction.

In the $3S_U$ to $3S_F$ transition in the structural homologue ONC, only one $3S_F$ species is populated, des-[30−75] (*22*), which is structurally homologous to des-[40−95] in RNase A. In the native structure of ONC, Y92 is replaced with R73 which does not participate in any interaction that would shield this disulfide bond (*23*). In fact, the (30−75) disulfide bond is approximately 4 times more exposed in ONC than the (40−95) disulfide bond in RNase A (*23*). Therefore, as ONC undergoes the $3S_U$ to $3S_F$ transition, the (30−75) disulfide bond is the least protected and thus cannot stabilize a $3S_F$ species other than des-[30−75].

In the conformational folding pathway of disulfide-bond-sintact RNase A, the loss of this ring-stacking interaction does not affect other interactions that are required for U-RNase A to fold; the time constants and amplitudes of the other phases for the Y92 mutants and wild-type RNase A listed in Table 2 are virtually unchanged by the removal of this ring-stacking interaction. Therefore, there are enough interactions other than the ring-stacking interaction of P93 and Y92 for RNase A to fold into its biologically active form.

By observing how the removal of a tyrosyl−prolyl stacking interaction affects the oxidative folding and disulfide-intact conformational folding of RNase A, we demonstrate how native interactions become more important along a folding pathway when SH/S−S reshuffling is allowed to occur. This reshuffling allows more conformational freedom in the backbone during a folding pathway; as a result, more favorable interactions between the side chains are required as the native structure is formed.

REFERENCES

1. Brems, D. N., and Baldwin, R. L. (1985) Protection of amide protons in folding intermediates of ribonuclease A measured by pH-pulse exchange curves. *Biochemistry 24*, 1689–1693.
2. Wearne, S. J., and Creighton, T. E. (1988) Further experimental studies of the disulfide folding transition of ribonuclease A. *Proteins 4*, 251–261.
3. Laurents, D. V., Bruix, M., Jamin, M., and Baldwin, R. L. (1998) A pulse-chase-competition experiment to determines if a folding intermediate is on or off-pathway: Application to ribonuclease A. *J. Mol. Biol. 3*, 669–678.
4. Ruoppolo, M., Vinci, F., Klink, T. A., Raines, R. T., and Marino, G. (2000) Contribution of individual disulfide bonds to the oxidative folding of ribonuclease A. *Biochemistry 39*, 12033–12042.
5. Houry, W. A., Rothwarf, D. M., and Scheraga, H. A. (1994) A very fast phase in the refolding of disulfide-intact ribonuclease A: Implications for the refolding and unfolding pathways. *Biochemistry 33*, 2516–2530.

6. Dodge, R. W., and Scheraga, H. A. (1996) Folding and unfolding kinetics of the proline-to-alanine mutants of bovine pancreatic ribonuclease A. *Biochemistry 35*, 1548–1559.
7. Houry, W. A., Rothwarf, D. M., and Scheraga, H. A. (1996) Circular dichroism evidence for the presence of burst-phase intermediates on the conformational folding pathway of ribonuclease A. *Biochemistry 35*, 10125–10133.
8. Rothwarf, D. M., Li, Y.-J., and Scheraga, H. A. (1998) Regeneration of bovine pancreatic ribonuclease A: Identification of two native-like three-disulfide intermediates involved in separate pathways. *Biochemistry 37*, 3760–3766.
9. Rothwarf, D. M., Li, Y.-J., and Scheraga, H. A. (1998) Regeneration of bovine pancreatic ribonuclease A: Detailed kinetic analysis of two independent folding pathways. *Biochemistry 37*, 3767–3776.
10. Schmid, F. X., and Baldwin, R. L. (1978) Acid catalysis of the formation of the slow-folding spcies of RNase A: Evidence that the reaction is proline isomerization. *Proc. Natl. Acad. Sci. U.S.A. 75*, 4764–4768.
11. Schultz, D. A., Schmid, F. X., and Baldwin, R. L. (1992) Cis proline mutants of ribonuclease A. II. Elimination of the slow-folding forms by mutation. *Protein Sci. 1*, 917–924.
12. Lueng, H., Xu, G., Narayan, M., and Scheraga, H. A. (2005) Impact of an easily reducible disulfide bond on the oxidative folding rate of multi-disulfide-containing proteins. *J. Pept. Res. 65*, 47–54.
13. Xu, G., Narayan, M., Kurinov, I., Ripoll, D., Welker, E., Khalili, M., Ealick, S. E., and Scheraga, H. A. (2006) A localized specific interactions alters the unfolding pathways of structural homologs. *J. Am. Chem. Soc. 128*, 1204–1213.
14. Wlodawer, A., Svensson, L. A., Sjoelin, L., and Gilliland, G. L. (1988) Structure of phosphate-free ribonuclease A refined at 1.26 Å. *Biochemistry 27*, 2705–2717.
15. Li, Y.-J., Rothwarf, D. M., and Scheraga, H. A. (1995) Mechanism of reductive protein unfolding. *Nat. Struct. Biol. 6*, 489–494.
16. Cao, A., Welker, E., and Scheraga, H. A. (2001) Effect of mutation of proline 93 on redox unfolding/folding of bovine pancreatic ribouclease A. *Biochemistry 40*, 8536–8541.
17. Shimotakahara, S., Rios, C. B., Laity, J. H., Zimmerman, D. E., Scheraga, H. A., and Montelione, G. T. (1997) NMR structural analysis of an analog of an intermediate formed in the rate-determining step of one pathway in the oxidative folding of bovine pancreatic ribonuclease A: Automated analysis of ^{1}H, ^{13}C, and ^{15}N resonance assignments for wild-type and [C65S, C72S] mutant forms. *Biochemistry 36*, 6915–6929.
18. Laity, J. H., Lester, C. C., Shimotakahara, S., Zimmerman, D. E., Montelione, G. T., and Scheraga, H. A. (1997) Structural characterization of an analog of the major rate-determining disulfide folding intermediate of bovine pancreatic ribonuclease A. *Biochemistry 36*, 12683–12699.
19. Laity, J. H., Shimotakahara, S., and Scheraga, H. A. (1993) Expression of wild-type and mutant bovine pancreatic ribonuclease A in *Escherichia coli*. *Proc. Natl. Acad. Sci. U.S.A. 90*, 615–619.
20. Wu, J., and Watson, J. T. (1997) A novel methodology for assignment of disulfide bond pairings in proteins. *Protein Sci. 6*, 391–398.
21. Pradeep, L., Kurinov, I., Ealick, S. E., and Scheraga, H. A. (2007) Implementation of a k/k_0 method to identify long-range structure in transition states during conformational folding/unfolding of proteins. *Structure 15*, 1178–1189.
22. Xu, G., Narayan, M., Welker, E., and Scheraga, H. A. (2004) Characterization of the fast-forming intermediate, des-[30−75] in the reductive unfolding of onconase. *Biochemistry 43*, 3246–3254.
23. Narayan, M., Xu, G., Ripoll, D. R., Zhai, H., Breuker, K., Wanjalla, C., Leung, H. J., Navon, A., Welker, E., McLafferty, F. W., and Scheraga, H. A. (2004) Dissimilarity in the reductive unfolding pathways of two ribonuclease homologs. *J. Mol. Biol. 338*, 795–809.